Deep Learning for RF-based Drone Detection and Identification using Welch's Method

Mahmoud Almasri[a]
LABSTICC, UMR 6285 CNRS, ENSTA Bretagne, 2 rue F. Verny, 29806 Brest Cedex 9, France

Keywords: Artificial Intelligence, Deep Neural Network, Drone Identification and Classification, Welch.

Abstract: Radio Frequency (RF) combined with the deep learning methods promised a solution to detect the presence of the drones. Indeed, the classical techniques (i.e. radar, vision and acoustics, etc.) suffer several drawbacks such as difficult to detect the small drones, false alarm of flying birds or balloons, the influence of the wind on the performance, etc. For an effective drones's detection, two main stages should be established: Feature extraction and feature classification. The proposed approach in this paper is based on a novel feature extraction method and an optimized deep neural network (DNN). At first, we present a novel method based on Welch to extract meaningful features from the RF signal of drones. Later on, three optimized Deep Neural Network (DNN) models are considered to classify the extracted features. The first DNN model can be used to detect the presence of the drones and contains two classes. The second DNN help us to detect and recognize the type of the drone with 4 classes: A class for each drone and the last one for the RF background activities. In the third model, 10 classes have been considered: the presence of the drone, its type, and its flight mode (i.e. Stationary, Hovering, flying with or without video recording). Our proposed approach can achieve an average accuracy higher than 94% and it significantly improves the accuracy, up to 30%, compared to existing methods.

1 INTRODUCTION

Tackling malicious and dangerous Unmanned Aerial Vehicles (UAVs) use requires the parallel development of systems capable of detecting, tracking and recognizing UAVs in an automatic and non-collaborative way. Indeed, the development of drones and the threats for sensitive sites make their detection and identification critical. It is therefore necessary to develop robust, reliable and inexpensive solutions to locate and identify these drones. Several modalities are available to deal with this problem, such as optical or radar imagery, the detection of Radio-Frequency (RF) communications or even acoustics. In (Bernardini et al., 2017), acoustic drone localization and detection has been proposed using support vector machines. In (Chang et al., 2018; Busset et al., 2015), the authors propose to use the acoustic cameras methodology to detect and identify the drones. Video detection is also possible but quickly limited by the particular experimental conditions (Ramamonjy et al., 2016). However, very high performance cameras should be dedicated to this task, and require an initial localization step to be able to target the drone beforehand. In (Bisio et al., 2018), Radar imagery shows limited performance due to little reflected radar signal portion that mainly depends on the stealth technology.

RF signal emitted from UAVs is recently attracted more attention to detect malicious drones and is suited to be used in several scenarios (Azari et al., 2018). This methodology is nor depends on the used wireless technologies of drones such as Wi-Fi, Bluetooth, 4G, etc. RF combined with the Deep Neural Network (DNN) may provide a more effective solution for drones detection and classification. However, the DNN model is widely suggested in several fields such as speech recognition (Chan et al., 2016; Graves et al., 2013), signal compression (Al-Sa'D et al., 2018), and in other fields (LeCun et al., 2015).

The DNN model has emerged as the most important and popular Artificial Intelligence (AI) technique (Deng et al., 2018; Zhao and Gao, 2019).
In this paper, the two main challenges for drones detection and identification are suggested: feature extraction and feature classification. The aim of feature extraction is to get a low dimensional representation of the data without losing information of the original data space. Then, the complexity of the data is re-

[a] https://orcid.org/0000-0002-9106-4020

Almasri, M.
Deep Learning for RF-based Drone Detection and Identification using Welch's Method.
DOI: 10.5220/0010530302080214
In *Proceedings of the 10th International Conference on Data Science, Technology and Applications (DATA 2021)*, pages 208-214
ISBN: 978-989-758-521-0

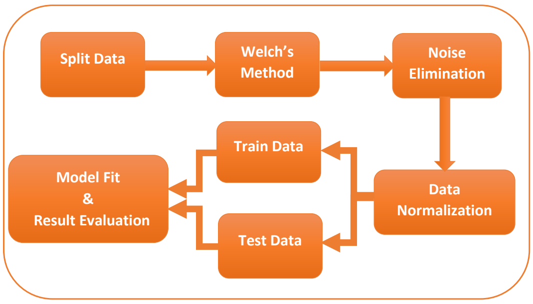

Figure 1: Flowchart of the entire process.

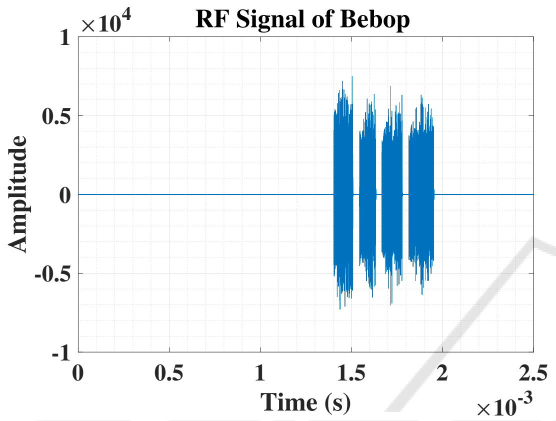

Figure 2: One segment of Bebop RF signal.

duced to a simple representation.

The second challenge, to classify the features vector gathered from the feature extraction stage in which the classification in this work is performed using the DNN model. Generally, the classification with a low feature dimension can accelerate the model speed and limit storage requirements. In this work, three DNN models are developed:

- To detect the presence of a drone.
- To detect the presence of a drone, and identify its type.
- To detect the presence of a drone, identify its type, and finally determine its flight mode.

2 PROPOSED APPROACH FOR FEATURE EXTRACTION

In this section, we present our proposed approach to extract meaningful features, and prepare the dataset for classification using an optimized DNN model. We use an open access dataset of (Al-Sa'd et al., 2019), that contains RF signals for three drones: Parrot Bebop, Parrot AR, and DJI Phantom 3. In (Al-Sa'd et al., 2019), the acquisition is performed under differ-

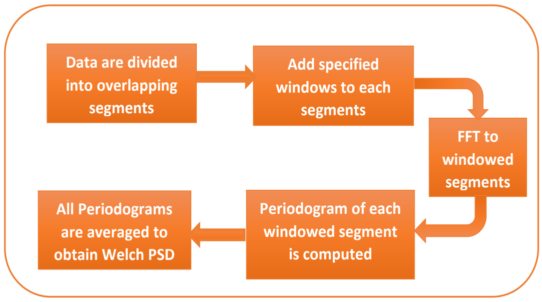

Figure 3: Welch PSD algorithm.

ent modes: drones are off (i.e. Background activity), on and connected, hovering, flying with and without video recording.

Fig. 1 shows a flowchart of the entire proposed approach. At first, all data are split into small segments (e.g. of 2.5 ms) in order to obtain a large amount of the data that are required to train and test the DNN model. Fig. 2 represents a segment of the obtained signal of Parrot Bebop.

For $Fs = 40MHz$, the number of samples in Fig. 2 (also in each segment) is 10^5 sample. In order to extract the most important features and reduce the number of samples in each segment, we focus on Welch's method.

Indeed, Welch represents one of the most popular method to calculate the Power Spectral Density (PSD) for a given signal (Jahromi et al., 2018). Using Welch's method, on the one hand, can significantly decrease the number of the features in the dataset; otherwise, the DNN model will be trained for too long time, and that may cause the model overfitting. On the other hand, it is necessary to discard the noise segments, that provide a low power; otherwise, the accuracy will be significantly decreased because the noise segments are used to train and test the DNN model[1]. To perform Welch spectral analysis, Fig. 3 shows the different stages of the Welch's method. Let us begin to divide a given signal x into N sample: $x[0], x[1], \ldots, x[N-1]$. Then, all samples are splitted into K overlapping segments that is considered, in most cases, equal to 50%. Let M be the length of each segment, N is the total number of segments, and S is the number of samples to shift between segments. Then, we obtain:

[1] In our DNN model, there is a class for the noise (RF background activities) in order to train the DNN model to differentiate the signal of the drone from the noise. Then, if all classes contain noise segments, the accuracy will be significantly decreased as in the case of (Al-Sa'd et al., 2019).

Segment 1: $x[0], x[1], \ldots, x[M-1]$
Segment 2: $x[S], x[S+1], \ldots, x[M+S-1]$

.
.
.

Segment K: $x[N-M], x[N-M+1], \ldots, x[N-1]$

For each segment $k = 1, \ldots, K$, compute a windowed Discrete Fourier Transform (DFT) as follows:

$$X_k(f) = \sum_m x[m]w[m]\exp\left(-\frac{2\pi f j}{M}m\right) \quad (1)$$

where $m = (k-1)S, \ldots, M + (k-1)S - 1$ and $w[m]$ represents the window function. Then, calculate the periodogram $P_k(f)$ for each segment as follows:

$$P_k(f) = \frac{1}{W}|X_k(f)|^2 \quad (2)$$

where $W = \sum_m w^2[m]$. Finally, average the periodogram for each segments to obtain Welch's PSD:

$$S_k(f) = \frac{1}{K}\sum_{k=1}^{K} P_k(f) \quad (3)$$

After splitting the data and applying Welch's method on all segments, a threshold γ is established in order to eliminate all segments with a low PSD[2]. Tab. 1 represents all segments in each class before and after eliminate noise segments that have a PSD lower than the threshold γ. To finalize the data preparation, all segments should be normalized in order to make sure that the different segments take on similar ranges of values. Then, the necessary time to train the DNN model is reduced while still providing the most accurate results (Passalis et al., 2019). In (Sola and Sevilla, 1997), the authors show that the best normalization method can be achieved when all segments are in the same magnitude, and specially if they are in the order of one. For this reason, after noise elimination, all segments are normalized using the min-max method that provides better results in most object classification (Al Shalabi et al., 2006; Saranya and Manikandan, 2013):

$$x = \frac{x - \min(x)}{\max(x) - \min(x)} \quad (4)$$

After performing Welch's method and the segment normalization on the signal of the Bebop in Fig. 2, we obtain Fig. 4.

[2]This threshold level can be chosen with respect to the RF background activities where there is no-drone signal.

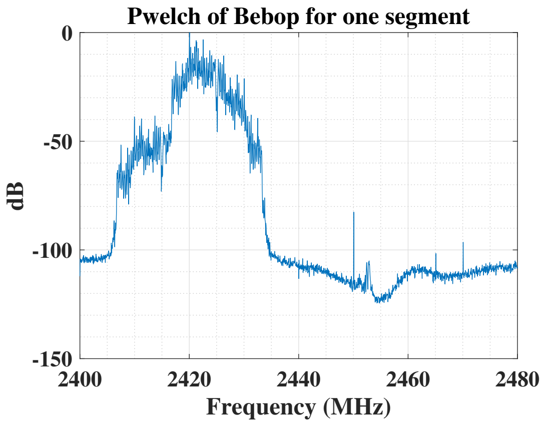

Figure 4: Welch based estimates, Hamming window, 2050 samples long segment, 50% overlap, min-max normalization.

3 DEEP NEURAL NETWORK MODEL

Deep Neural Network (DNN) has shown surpassing results in various cognitive tasks such as speech recognition, object detection and identification, etc. At first, we present the DNN concept and general architecture. Later on, we optimize the architecture of the DNN model in order to accelerate the training time and also to achieve a better accuracy. A DNN model has an input layer, hidden layers and an output layer. For a given DNN model, the mathematical input-output relationship can be expressed as follows(He and Xu, 2010):

$$z_k^l = f^l(W^l z_k^{(l-1)} + b^l), \quad (5)$$

$$W^{(l)} = \begin{bmatrix} w_{11}^{(l)} & w_{12}^{(l)} & \cdots & w_{1H^{(l-1)}}^{(l)} \\ w_{21}^{(l)} & w_{22}^{(l)} & \cdots & w_{2H^{(l-1)}}^{(l)} \\ \vdots & \vdots & \ddots & \vdots \\ w_{H^{(l)}1}^{(l)} & w_{H^{(l)}2}^{(l)} & \cdots & w_{H^{(l)}H^{(l-1)}}^{(l)} \end{bmatrix} \quad (6)$$

z_k^l is the output of layer l and the input to layer $l+1$ for the k^{th} segment; $z_k^{(l-1)}$ represents the output of layer $(l-1)$ and the input to layer l; for instance, z_k^0 stands for the k^{th} segment at the input layer and z_k^L represents the classification vector for the k^{th} segment where L is the output layer; f^l is the activation function of layer l; This later can be any linear or non-linear function, such as: the rectified linear unit (ReLU), Sigmoid, Softmax, TanH, etc. W^l is the weight matrix of layer l; w_{pq}^l is the weight between the p^{th} neuron of layer l and the q^{th} neuron of layer $l-1$; $b^l = [b_1^l, b_2^l, \ldots, b_{(H^l)}^l]$ is the bias vector of layer

Table 1: Class Labels, Acronyms, and Class Sample Rate before and after the Preprocessing.

Classes	Class Name	Acronyms	nb. of segments before the preprocessing	nb. of segments after the preprocessing
1	No-Drone (Background activities)	ND	4100	4100
2	Bebop Static	BS	2100	832
3	Bebop Hovering	BH	2100	695
4	Bebop Flying	BF	2100	720
5	Bebop Flying & Video recording	BFV	2100	696
6	AR Static	AS	2100	659
7	AR Hovering	AH	2100	526
8	AR Flying	AF	2100	566
9	AR Flying & Video recording	AFV	1800	886
10	Phantom Static	PS	2100	1627

l; H^l is the total number of neurons in layer l; for instance, H^0 is the number of features at the input and H^L is the number of classes in the classification vector at the output.

3.1 DNN Model Optimization

In a DNN model, the weight and biases are updated through a supervised learning process with respect to minimizing the classification error (Bottou, 2010). Several classification loss functions are adapted to DNN models and widely used in the literature, such as Mean Square Error (MSE), cross-entropy, etc. Cross-entropy is the most commonly used loss function for multi-class classification problems (Nielsen, 2015), (Zhu et al., 2020) and (Nasr et al., 2002). Cross-entropy for a multi-class classification task measures the dissimilarity between the target label distribution y_j and the predicted one $\hat{y}_j$, and can be expressed as follows:

$$L(y_j, \hat{y}_j) = -\sum_{j=1}^{C} y_j log(\hat{y}_j) \tag{7}$$

In eq. (7), the Cross-entropy is configured with C class ($C = H^L$), and a 'Softmax' activation function should be used at the output layer in order to predict the probability for each class (Liu et al., 2016; Kobayashi, 2019; Agarwala et al., 2020). While for hidden layers, we use the rectified linear unit (ReLU) that represents the most used activation function by default for performing a majority of the deep learning tasks. Softmax and ReLU functions are respectively expressed in eq. (8) and (9):

$$f(x_i) = \frac{e^{x_i}}{\sum_{j=1}^{C} e^{x_j}}, \text{for } i\text{=1,...,}C \tag{8}$$

$$f(x_i) = \begin{cases} x_i & x_i > 0 \\ 0 & x_i \leq 0 \end{cases} \tag{9}$$

Let's start to determine the best number of layers and neurons in the hidden layers. For the input layer, the number of neurons is equal to 2050 that represents the number of samples in each segment. While the number of neurons at the output is equal to 2, 4 or 10 classes for the first, second, and third DNN model. For hidden layers, until now, there were no-definitive rules for choosing the number of hidden layers, and the best number of neurons in each hidden layer. Several methods are used without providing an exact formula for determining the number of hidden layers as well as the number of neurons in each hidden layer. For the number of hidden layers, the best hidden layers is achieved when the number of layers ranges from 1-5 (Arifin et al., 2019). However, adding more unnecessary hidden layer can significantly increase the complexity of the network.

For the number of neurons in hidden layers, several works attempt different methods trying to maximize the model accuracy, and some rules are suggested:

- The required hidden neurons are $\frac{2}{3}$ (or from 70% to 90%) of the size of the input layer (Boger and Guterman, 1997).
- The number of hidden neurons should be less than twice of the number of neurons in the input layer (Berry and Linoff, 2004).
- The number of hidden neurons can be as high as the number of training segments (Huang, 2003).
- The number of hidden neurons should be between the input layer neurons and the output layer ones (Blum, 1992).

Based on the above discussion, and to reduce the complexity of the DNN model, we consider three layers with the following number of neurons: 256, 128 and 64.

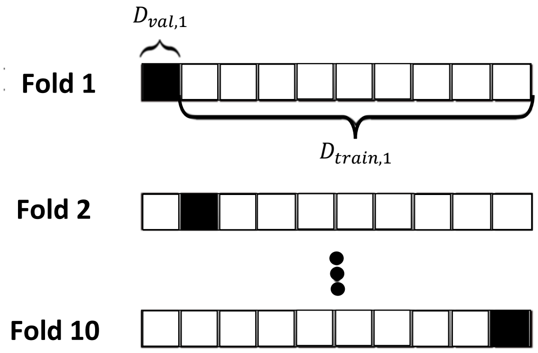

Figure 5: 10-fold cross-validation. The data is randomly partitioned into 10 blocks, each of them contains 10% of the data. 90% of the data are used to train the model training and 10% for model validation.

3.2 K-fold Cross-Validation

K-fold Cross-Validation represents one of the most used technique for model evaluation in machine learning practice. However, machine learning models sometimes cannot generalize well on unseen data that has not been trained yet. To ensure that the model is relevant and can perform well on new data, K-fold Cross-Validation is recommended. As well, it ensures that all RF segments in the dataset has the same chance to be in training and test set. In K-fold Cross-Validation, RF segments are divided into K blocks with equal size. Then, one block is used for the validation while the other $K-1$ blocks contribute to train the DNN model, and a validation performance can be calculated. The operation is repeated K times, by selecting another validation block, in order to obtain a model that have both low bias and variance. The global cross-validated performance can be obtained by averaging the K performance measurements.

Fig. 5 illustrates the K-fold cross validation for $K = 10$ where $D_{val,1}$ in the first fold represents the data validation and blocks $D_{train,1}$ serve as training data. In (Raschka, 2018), the experiments show that $K = 10$ represents a good choice for K.

4 RESULTS AND DISCUSSION

In this section, we use several metrics in order to evaluate the performance of our proposed method: Accuracy, Precision, recall, error, false discovery rate (FDR), false negative rate (FNR) and F1 scores via confusion matrices. These metrics are defined as follows:

$$\text{Accuracy} = \frac{TP+TN}{TP+TN+FP+FN} \tag{10}$$

$$\text{Precision} = \frac{TP}{TP+FP} \tag{11}$$

$$\text{Recall} = \frac{TP}{TP+FN} \tag{12}$$

$$\text{Error} = 1 - \text{Accuracy} \tag{13}$$

$$\text{FDR} = 1 - \text{Precision} \tag{14}$$

$$\text{FNR} = 1 - \text{Recall} \tag{15}$$

where TP, TN, FP and FN are true positives, true negatives, false positives and false negatives respectively. We develop three DNNs models for drones detection and identification. The Confusion Matrix of the three DNN models for 2-class, 4-class and 10-class are respectively shown in Figs. 6a, 6b and 6c. In that figures, the rows of the inner 2x2, 4x4 and 10x10 matrices represent the predicted class while the columns correspond to the true class. The diagonal cells, exhibited in green, represent the number of segments that are correctly classified, while the red cells refer to the incorrectly classified segments. As well as, each cell show the number of segments and the percentage of the total number of segments. The gray cells in the right column show the precision and FDR in green and red respectively. Furthermore, the gray cells in the row at the bottom illustrate the recall in green, and FNR in red. In addition, the blue cell in the bottom right of the plot shows the overall accuracy in green, and the error in red. Moreover, the yellow column and row on the far left and top show the F1 scores for predicting each class in green and its complementary in red, (1-F1 score), for completeness. Finally, the orange cell in the upper left of the plot shows the averaged F1 score for all classes in green and its complementary in red. The first DNN model in Fig. 6a, for two classes, shows that the average accuracy is about of 99.7%, average error of 0.3% and average F1 score of 99.7%. Fig. 6b depicts the classification performance of the second DNN model, which detects the presence of a drone and identifies its type. Results demonstrate an average accuracy of 97.7%, average error of 2.3%, and average F1 score of 97.5%.

We should notice that the average accuracy is significantly improved using our approach based on Welch's method compared to the proposed methods in (Al-Sa'd et al., 2019; Al-Emadi and Al-Senaid, 2020; Allahham et al., 2020). Indeed, the achieved accuracies in the latter references, for 4 classes, are respectively: 84.5%, 85.8 % and 94.6 %.

Finally, Fig. 6c illustrates the classification performance of the third DNN model which detects the presence of a drone, identifies its type, and determines its flight mode. Results demonstrate an average accuracy of 94.5%, average error of 5.5%, and average

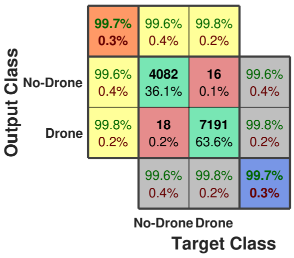

(a) Confusion Matrix of the first DNN model

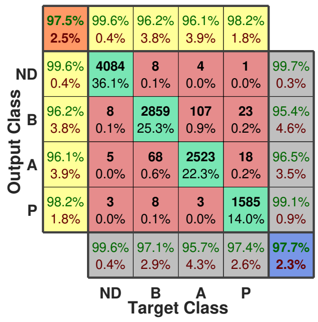

(b) Confusion Matrix of the second DNN model

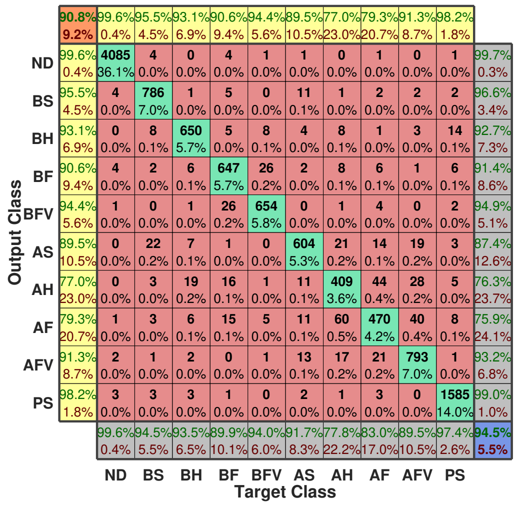

(c) Confusion Matrix of the third DNN model

Figure 6: Confusion matrix of the three DNN models. Fig. 6a represents two classes: No-Drone and Drone. Fig. 6b depicts the performance of the second DNN model for 4 classes: ND (No-drone), B (Bebop), A (AR) and P (Phantom). The Acronyms in Fig. 6c are shown in Tab. 1.

F1 score of 90.8%. While, the obtained accuracies in (Al-Sa'd et al., 2019; Al-Emadi and Al-Senaid, 2020; Allahham et al., 2020) are respectively: 46.8%, 59.2% and 87.4%. Then, the average accuracy of our proposed method, for 10 classes, can be greatly enhanced by 47%, 35% and 7% compared to the proposed methods in the latter references.

5 CONCLUSION

In Intelligent detection and identification techniques have emerged vastly by the rise of data driven algorithms, such as neural networks. In the Deep Neural Network (DNN), extracting features from given data represents a critical importance for the successful application of machine learning. In this work, we proposed a novel approach based on Welch's method for feature extraction in order to enhance the classification performance of multi-class and maximize the average accuracy. Using Welch's method, the number of extracted features at the input of the DNN model can be reduced. Moreover, it can estimate if a given segment of data contains an useful information or not, so that the noise segments can be eliminated. Three DNN models have been used to classify the extracted features, and then detect the presence of a drone, identify its type and finally determine its flight mode. In the first DNN model, for two classes, the achieved average accuracy is about of 99.7%. By increasing the number of classes in the second DNN model, 4 classes are used, the average accuracy is slightly decreased to 97.7%. In the last DNN model with 10 classes, the obtained accuracy is about of 94.5% that is enhanced up to 47% compared to existing methods.

In the future work, another important feature extraction methods can be used in the frequency or time domains, such as Entropy, Skewness, kurtosis, etc. Another potential research direction is to apply another powerful machine learning technologies to address the fundamental visual feature extraction issue.

REFERENCES

Agarwala, A., Pennington, J., Dauphin, Y., and Schoenholz, S. (2020). Temperature check: theory and practice for training models with softmax-cross-entropy losses. *arXiv preprint arXiv:2010.07344*.

Al-Emadi, S. and Al-Senaid, F. (Doha, Qatar, February, 2020). Drone detection approach based on radio-frequency using convolutional neural network. In *IEEE International Conference on Informatics, IoT, and Enabling Technologies*, pages 29–34.

Al-Sa'd, M. F., Al-Ali, A., Mohamed, A., Khattab, T., and Erbad, A. (2019). Rf-based drone detection and identification using deep learning approaches: An initiative towards a large open source drone database. *Future Generation Computer Systems*, 100:86–97.

Al-Sa'D, M. F., Tlili, M., Abdellatif, A. A., Mohamed, A., Elfouly, T., Harras, K., O'Connor, M. D., et al. (2018). A deep learning approach for vital signs compression and energy efficient delivery in mhealth systems. *IEEE Access*, 6:33727–33739.

Al Shalabi, L., Shaaban, Z., and Kasasbeh, B. (2006). Data mining: A preprocessing engine. *Journal of Computer Science*, 2(9):735–739.

Allahham, M. S., Khattab, T., and Mohamed, A. (Doha, Qatar, February, 2020). Deep learning for rf-based drone detection and identification: A multi-channel 1-d convolutional neural networks approach. In *IEEE International Conference on Informatics, IoT, and Enabling Technologies*, pages 112–117.

Arifin, F., Robbani, H., Annisa, T., and Ma'arof, N. (2019). Variations in the number of layers and the number of neurons in artificial neural networks: Case study of pattern recognition. In *Journal of Physics: Conference Series*, volume 1413, page 012016.

Azari, M. M., Sallouha, H., Chiumento, A., Rajendran, S., Vinogradov, E., and Pollin, S. (2018). Key technologies and system trade-offs for detection and localization of amateur drones. *IEEE Communications Magazine*, 56(1):51–57.

Bernardini, A., Mangiatordi, F., Pallotti, E., and Capodiferro, L. (2017). Drone detection by acoustic signature identification. *Electronic Imaging*, 2017(10):60–64.

Berry, M. J. and Linoff, G. S. (2004). *Data mining techniques: for marketing, sales, and customer relationship management*. John Wiley & Sons.

Bisio, I., Garibotto, C., Lavagetto, F., Sciarrone, A., and Zappatore, S. (2018). Blind detection: Advanced techniques for wifi-based drone surveillance. *IEEE Transactions on Vehicular Technology*, 68(1):938–946.

Blum, A. (1992). *Neural networks in C++: an object-oriented framework for building connectionist systems*. John Wiley & Sons, Inc.

Boger, Z. and Guterman, H. (Orlando, FL, USA, October, 1997). Knowledge extraction from artificial neural network models. In *IEEE International Conference on Systems, Man, and Cybernetics, Computational Cybernetics and Simulation*, volume 4, pages 3030–3035.

Bottou, L. (Paris France, August, 2010). Large-scale machine learning with stochastic gradient descent. In *International Conference on Computational Statistics*.

Busset, J., Perrodin, F., Wellig, P., Ott, B., Heutschi, K., Rühl, T., and Nussbaumer, T. (2015). Detection and tracking of drones using advanced acoustic cameras. In *Unmanned/Unattended Sensors and Sensor Networks XI; and Advanced Free-Space Optical Communication Techniques and Applications*, volume 9647, page 96470.

Chan, W., Jaitly, N., Le, Q., and Vinyals, O. (Shanghai, China, March, 2016). Listen, attend and spell: A neural network for large vocabulary conversational speech recognition. In *IEEE International Conference on Acoustics, Speech and Signal Processing*.

Chang, X., Yang, C., Wu, J., Shi, X., and Shi, Z. (Sheffield, UK, July, 2018). A surveillance system for drone localization and tracking using acoustic arrays. In *IEEE Sensor Array and Multichannel Signal Processing Workshop (SAM)*.

Deng, C., Liao, S., Xie, Y., Parhi, K. K., Qian, X., and Yuan, B. (Fukuoka, Japan, October, 2018). Permdnn: Efficient compressed dnn architecture with permuted diagonal matrices. In *Annual IEEE/ACM International Symposium on Microarchitecture (MICRO)*.

Graves, A., Abdelrahman, M., and Hinton, G. (Vancouver, Canada, 2013). Speech recognition with deep recurrent neural networks.

He, X. and Xu, S. (2010). Artificial neural networks. *Process neural networks: theory and applications*, pages 20–42.

Huang, G.-B. (2003). Learning capability and storage capacity of two-hidden-layer feedforward networks. *IEEE Transactions on Neural Networks*, 14(2):274–281.

Jahromi, M. G., Parsaei, H., Zamani, A., and Stashuk, D. W. (2018). Cross comparison of motor unit potential features used in emg signal decomposition. *IEEE Transactions on Neural Systems and Rehabilitation Engineering*, 26(5):1017–1025.

Kobayashi, T. (Cardiff, UK, September, 2019). Large margin in softmax cross-entropy loss. In *British Machine Vision Conference*.

LeCun, Y., Bengio, Y., and Hinton, G. (2015). Deep learning. *nature*, 521(7553):436–444.

Liu, W., Wen, Y., Yu, Z., and Yang, M. (New York City, USA, June, 2016). Large-margin softmax loss for convolutional neural networks. In *International Conference on Machine Learning*.

Nasr, G. E., Badr, E., and Joun, C. (2002). Cross entropy error function in neural networks: Forecasting gasoline demand. In *FLAIRS conference*, pages 381–384.

Nielsen, M. A. (2015). *Neural networks and deep learning*, volume 2018. Determination press San Francisco, CA.

Passalis, N., Tefas, A., Kanniainen, J., Gabbouj, M., and Iosifidis, A. (2019). Deep adaptive input normalization for time series forecasting. *IEEE Transactions on Neural Networks and Learning Systems*.

Ramamonjy, A., Bavu, E., Garcia, A., and Hengy, S. (Le Mans, France, 2016). Détection, classification et suivi de trajectoire de sources acoustiques par captation pression-vitesse sur capteurs mems numériques. In *Congrès de la Société Française d'Acoustique-CFA16/VISHNO*.

Raschka, S. (2018). Model evaluation, model selection, and algorithm selection in machine learning. *arXiv preprint arXiv:1811.12808*.

Saranya, C. and Manikandan, G. (2013). A study on normalization techniques for privacy preserving data mining. *International Journal of Engineering and Technology*, 5(3):2701–2704.

Sola, J. and Sevilla, J. (1997). Importance of input data normalization for the application of neural networks to complex industrial problems. *IEEE Transactions on nuclear science*, 44(3):1464–1468.

Zhao, C. and Gao, X.-S. (2019). Qdnn: Dnn with quantum neural network layers. *arXiv preprint arXiv:1912.12660*.

Zhu, Q., He, Z., Zhang, T., and Cui, W. (2020). Improving classification performance of softmax loss function based on scalable batch-normalization. *Applied Sciences*, 10(8):2950.